A Kinetic Model for Diffusion-Controlled Bulk Cross-Linking Photopolymerizations

Devdatt L. Kurdikar and Nikolaos A. Peppas*

School of Chemical Engineering, Purdue University, West Lafayette, Indiana 47907-1283

Received December 16, 1993; Revised Manuscript Received May 2, 1994®

ABSTRACT: A mean-field kinetic model was developed to describe a diffusion-controlled bulk cross-linking photopolymerization. This model incorporates all the physical transport limitations that directly or indirectly affect polymerization parameters and rate constants in such reactions. Events such as the continuous decrease in initiator efficiency and the presence of a temporary excess free volume were accounted for in the model development. Rate equations were written for each of the species present in the reacting system. The initiator efficiency was calculated throughout the reaction using a model previously developed by us. The propagation rate constant was calculated using the Smoluchowski rate expression and the Vrentas–Vrentas theory. Radical mobility caused by propagation diffusion was incorporated in the calculation of the termination rate constant. Where the values of model parameters were not available, typical values were calculated using predictive methods or group contribution methods. The model was able to predict kinetic results of diethylene glycol diacrylate photopolymerizations.

Introduction

Bulk polymerizations of multifunctional monomers lead to the formation of highly cross-linked polymer networks. These networks have found applications in the coatings, films, and packaging industries, in information technology,[1-3] and as biomaterials.[4-6] They are typically prepared by free-radical photopolymerizations since UV initiation affords good spatial and temporal control of the reaction.

Though the mechanism of such reactions is fairly well understood and well accepted, the kinetic modeling of the reaction process has proven to be somewhat difficult. This is because cross-linking homopolymerizations often exhibit tendencies that are not commonly observed in linear polymerizations. For example, the initiator efficiency, defined as the fraction of radicals produced that actually initiate propagating chains, usually lies between 0.3 and 0.8 for most systems at the start of the polymerization.[7] Studies using electron spin resonance (ESR) spectroscopy[8,9] to follow the radical concentration during polymerization demonstrate that the efficiency decreases continuously. In addition, previous studies[10] have shown the quasi-steady-state approximation for the radical concentration to be invalid. Radicals tend to get trapped when they are surrounded by polymer chains, and the space available for chain end movement is severely restricted.[11,12] Thus, in the polymerizing medium there coexist two dominant populations of radicals with different reaction tendencies: free radicals whose mobility is not directly restricted by spatial constraints and trapped radicals. Other reaction tendencies include strong autoacceleration at the onset of the polymerization[13] and final conversions significantly below 100%.[14]

These reaction trends are directly or indirectly caused by diffusional limitations on the mobility of the reacting species. Diffusional processes become important during the course of a linear polymerization, causing the controlling step of the reaction to shift from chemical reaction-controlled to diffusion-controlled. For a bulk cross-linking homopolymerization, diffusional limitations exist from the onset of the reaction, causing the reaction tendencies to be even more pronounced.

One of the most widely accepted models for the calculation of the diffusion-limited propagation and termination rate constants during linear polymerization has been developed by Marten and Hamielec.[15] Using the Doolittle equation for the diffusivity of a small molecule in a polymer solution, they derived expressions that could be used to calculate the rate constants throughout the range of conversion. These expressions have also been used in the modeling of cross-linking reactions;[10,16] however, a limitation of such an approach is the determination of the associated parameters used in the equations. Soh and Sundberg[17-20] used an approach similar to that of Marten and Hamielec for the calculation of the rate constants but also incorporated the mobility of the radicals due to the propagation reaction. Their model involved only two empirical constants but could not accurately predict limiting conversion.

More recent kinetic models for bulk cross-linking polymerizations have been offered by Chern and Poehlein[16] and Batch and Macosko.[21] The Chern and Poehlein (CP) model used a constant initiator efficiency and expressions for propagation and termination rate constants which involved parameters evaluated from fitting model results to experimental data. The Batch and Macosko (BM) model accounted for the diffusional effects on the reaction process. These investigators did include the changing initiator efficiency; however, it was done by employing an empirical expression. They assumed that the propagation rate constant was constant and that bimolecular termination was negligible. Kloosterboer has shown[1] that, during the course of the reaction, the volume shrinkage rate lags behind the reaction rate, leading to the presence of a temporary excess free volume which increases as the reaction rate is increased. Such a phenomenon which leads to an increase in the final conversion due to an increase in the reaction rate was not included in either of the models. In our estimation, the success of the previous models to predict the kinetic behavior is based to some extent on the use of a number of adjustable parameters.

Percolation models have also been developed to follow the kinetics of the cross-linking reaction as well as provide information on the structure of the network.[22,23] Some

* Corresponding author.
® Abstract published in *Advance ACS Abstracts*, June 15, 1994.

0024-9297/94/2227-4084$04.50/0

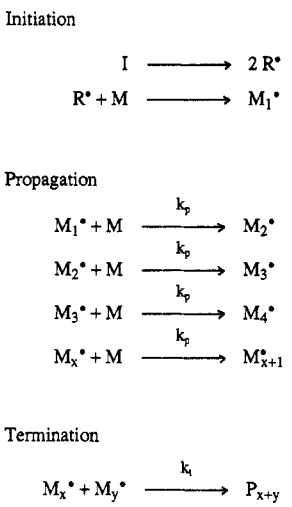

Figure 1. Typical free-radical polymerization reaction mechanism. The radical first decomposes into two radicals which can initiate chains by reaction with a monomer unit. In the propagation steps, monomer units are successively added to the active monomer to form a growing chain. Dead polymer chains are formed on the termination reaction of two growing chains.

recent advances in such models include the incorporation of varying initiation rate[24-27] and mobilities of the reacting species.[28,29] These models have proven useful in understanding the structural development of the network. However, at the present time, these models seem to have limited applicability for the prediction of the kinetic behavior of the crosslinking reaction.

In this paper, we present the derivation, simulation, and experimental verification of a kinetic model for the prediction of the reaction behavior of bulk multifunctional polymerizations. The model accounts explicitly for each of the physical processes that occur during the cross-linking reaction. Expressions were derived for the propagation and termination rate constants and incorporated into the rate equations, which were then numerically integrated to obtained the desired kinetic information. Using the previously reported[13] photopolymerization behavior of diethylene glycol diacrylate (DEGDA) as a model system, the simulated results were compared to experimental data.

Model Development

Free-radical photopolymerizations follow the typical chain reaction mechanism which is schematically shown in Figure 1. In the chain initiation step, the initiator splits up into two equal or unequal radicals which reacts with (meth)acryl groups to form active monomers. During propagation, the active monomers attach to unreacted monomers and form a growing polymer chain. Dead polymer chains are formed by the termination reaction in which two growing polymer chains react by a bimolecular mechanism. Chain-transfer reactions are assumed to be absent or suppressed. In the reaction scheme, R• is the primary radical produced on initiation decomposition, M is a monomer unit, M_i• is a growing polymer chain containing i monomers, P is a dead polymer chain, and k_p and k_t are the rate constants for the propagation and termination reactions, respectively.

These rate constants can take different values for different coexisting radical populations. However, for simplicity, the model presented in this paper uses single values for k_p and k_t. Also, it is assumed that termination is by combination only. Such an assumption is valid for acrylate polymerizations.[7] It must be noted that the traditional assumptions in the modeling of polymerization kinetics, such as the quasi-steady-state approximation (QSSA) for radical concentration, and a constant initiator efficiency throughout the polymerization process *were not made here.*

Based on the reaction scheme, rate equations were written for each of the species present in the reacting mixture. Expressions were then developed for the time-dependent initiator efficiency, k_p, and k_t, incorporating the volume relaxation using the Bowman and Peppas treatment.[10]

Rate Equations. For photoinitiated polymerizations, the rate of initiation, R_i, is given by[7]

$$R_i = 2\phi I_a \tag{1}$$

where I_a is the intensity of absorbed light and ϕ is the number of propagating chains produced per light photon absorbed (referred to as the quantum yield for initiation). The term ϕ was expressed as $\phi = f\phi'$ where f is the initiator efficiency and ϕ' is the number of initiator molecules dissociated per photon absorbed. The initiator efficiency is defined as the fraction of radicals produced that initiate propagating chains. The factor 2 accounts for the two radicals that are produced per initiator molecule.

The absorbed light intensity is often expressed[7] as

$$I_a = \epsilon I_0[A] \tag{2}$$

where ϵ is the extinction coefficient of the initiator, [A] is initiator concentration, and I_0 is the incident light intensity per unit area. This equation was written using the thin film approximation in the Beer–Lambert law which relates the absorbed light intensity to the incident light intensity.

Assuming bimolecular reaction, the rate of termination, R_t, could be calculated by

$$R_t = -2k_t[M^\bullet]^2 \tag{3}$$

where [M•] is the concentration of all polymer chain radicals in the system, and the factor 2 accounts for the destruction of two radicals per dead polymer chain formed.

Polymer radicals can be broadly classified into three populations: (i) free radicals that are not attached to the gel; (ii) radicals attached to the loosely cross-linked portion of the gel so that they are spatially restricted but still mobile; and (iii) trapped radicals which are surrounded by dead polymer chains and unable to react further. However, for simplicity, the various radical population concentrations were represented by an overall polymer radical concentration.

Then, the rate of change of radical concentration could be calculated from eq 1–3 as

$$d[M^\bullet]/dt = 2f\phi' I_0 \epsilon[A] - 2k_t[M^\bullet]^2 \tag{4}$$

The rate of polymerization, R_p, may be expressed as the rate of monomer loss[7]

$$R_p = -d[M]/dt = k_p[M][M^\bullet] \tag{5}$$

where [M] is the monomer concentration. This relation intrinsically assumes equal reactivity of the double bonds in an unreacted monomer unit and the pendant double bonds. The long-chain hypothesis is also made which implies that the loss of monomer units is primarily due to the propagation reaction and not by the chain initiation

reactions. This hypothesis is valid for a process that uses a low initiator concentration and produces high polymer.[7]

Initiator Efficiency. Most models assume that the initiator efficiency is constant throughout the polymerization process. Unfortunately, as the reaction medium becomes increasingly viscous, the reacting species' diffusivity drops considerably, and initiator recombination reactions become frequent. These lead to a drop in the value of the initiator efficiency. Shen *et al.*[9] reported that it approaches zero at limiting conversion. Thus, in the present work, the initiator efficiency was expressed as a function of the radical diffusivity and radical recombination reaction rate constants.

The initiator used in our work, 2,2-dimethoxy-2-phenylacetophenone, splits up into a benzoyl radical and a benzoylketal radical.[30-32] The latter further decomposes to form methyl benzoate and a methyl radical. The methyl and benzoyl radicals are instrumental in initiating chains. Recombination reactions of the methyl and benzoyl radicals, as well as the benzoyl and benzoylketal radicals, to form inactive molecules cause a decrease in the initiator efficiency. As the polymerization reaction proceeds and the diffusivity of the radicals drops, the recombination reactions have a greater probability of occurrence. Thus, the initiator efficiency decreases continuously during the course of polymerization.

Taking into account the various reactions that the radicals can undergo, an equation has been previously derived in our group[33] to relate the initiator efficiency to the diffusivity of the radicals in the polymerizing mixture.

$$f = \left[1 - \frac{ak_{i,1}}{D_A + ak_{i,1} + a(k_{d,r,1}D_A)^{1/2}}\right] \times \left[1 - \frac{b^2 k_{i,2} k_{d,r,1} \exp[(k_{d,r,1}/D_A)^{1/2}(a-b)]}{(\hat{k}/D_B)^{1/2} + (k_{d,r,1}/D_A)^{1/2}} \times \frac{1}{D_A + ak_{i,1} + a(k_{d,r,1}D_A)^{1/2}} \frac{1}{D_B + bk_{i,2} + b(\hat{k}D_B)^{1/2}}\right] \quad (6)$$

In this equation, f is the initiator efficiency, a and b are radii of the solvent cages around the two unequal primary radicals, $k_{i,1}$ is the specific intrinsic rate constant for the recombination of the benzoyl and the benzoylketal radicals, $k_{i,2}$ is the specific intrinsic rate constant for the recombination of the benzoyl and the methyl radicals, $k_{d,r,1}$ is the rate constant for the decomposition of the benzoylketal radical into methyl benzoate and the methyl radical, D_A is the relative diffusional constant for the benzoyl and the benzoylketal radical, and D_B is the relative diffusional constant for the methyl and the benzoyl radicals. The term $\hat{k}$ is expressed as

$$\hat{k} = k_{p,1}[M] + k_{t,1}[M^\cdot] \quad (7)$$

where $k_{p,1}$ is the true rate constant for the reaction of a primary radical with an unreacted monomer, and $k_{t,1}$ is the true rate constant for the reaction of a primary radical with a growing polymer chain.

Some observations can be made without loss of predictive abilities of this equation. All radicals have the same diffusivity and hence $D_A \approx D_B = 2D_r$ where D_r is the diffusion coefficient of a radical in the polymerizing mixture. In addition, the recombination reaction rate constants and the radii of the solvent cages were approximately equal so that $k_{i,1} \approx k_{i,2}$ and $a \approx b$. With these approximations, eq 6 becomes

$$f = \left[1 - \frac{ak_{i,1}}{D_A + ak_{i,1} + a(k_{d,r,1}D_A)^{1/2}}\right] \times \left[1 - \frac{a^2 k_{i,1} k_{d,r,1}}{(\hat{k}/D_A)^{1/2} + (k_{d,r,1}/D_A)^{1/2}} \times \frac{1}{D_A + ak_{i,1} + a(k_{d,r,1}D_A)^{1/2}} \frac{1}{D_A + ak_{i,1} + a(\hat{k}D_A)^{1/2}}\right] \quad (8)$$

Equation 8 has been shown[33] to have predictive abilities and does not involve any empirical constants or adjustable parameters. Also, as the reaction proceeds and the radical diffusion coefficient approaches a limiting value of zero, the initiator efficiency becomes zero. The term D_r was calculated continuously during the reaction process using the Vrentas and Vrentas theory[34] for diffusion of penetrants in lightly cross-linked polymers. In this manner, the continuous change in initiator efficiency was incorporated into the kinetic model.

Propagation. The propagation reaction involves the addition of a small monomer unit to a comparatively large growing chain. Such a process involves three steps. First, the monomer molecule must undergo translational diffusion toward the radical site. Then, the monomer must undergo segmental diffusion so that the reactive group is oriented toward the radical site and is accessible for propagation. Finally, a chemical reaction between the radical and the (meth)acryl group can occur. Such a reaction is typically diffusion-controlled in a bulk cross-linking polymerization. Also, the radical is usually present at a cross-link point in the network and possesses negligible mobility of its own as compared to the monomer diffusivity.

Since the translational and segmental diffusion processes occur in series, k_p can be represented by a sum of the reaction resistances as

$$\frac{1}{k_p} = \frac{1}{k_{p,trans}} + \frac{1}{k_{p,seg}} \quad (9)$$

where $k_{p,trans}$ is the translational contribution to the propagation rate constant and $k_{p,seg}$ is the segmental contribution to the propagation rate constant.

Diffusion-limited reactions can be treated using the Smoluchowski theory[35] which relates the reaction rate constant, k, to the relative diffusional coefficient of the reacting species, D, where R is the effective reaction radius.

$$k = 4\pi RD \quad (10)$$

This approach has been used as a basis for describing rate constants in polymerizing systems. For example, Tulig and Tirrell[36] and Ito[37,38] expressed the diffusion coefficient D in terms of the reptation theory and used eq 10 to calculate k_t.

Using the Smoluchowski rate expression for each of the translational and segmental contributions to k_p, we obtained

$$k_{p,trans} = 4\pi(r_m + r_r)D_m \quad (11)$$

$$k_{p,seg} = 4\pi(r_m + r_r)D_{seg} \quad (12)$$

where D_m is the translational diffusion coefficient and D_{seg} is the segmental diffusion coefficient of the monomer, and r_m and r_r are the reaction radii of the monomer and radical, respectively. The mobility of the radical was negligible in comparison to D_m and D_{seg}.

The translational diffusion coefficient of the monomer was estimated using the Vrentas and Vrentas extension[34] of the Vrentas and Duda diffusion theory.[39,40] This theory

is most suitable when there are at least 50 bond vectors between two cross-link points and hence in the modeling of the polymerizations of multifunctional monomers that have 50 bonds or more between the reactive groups.

The Vrentas–Duda theory for linear polymer–solvent systems relates the solvent self-diffusion coefficient, D_1, to the solvent and polymer mass fractions, ω_i, as follows:

$$D_1 = D_0 \exp\left[-\frac{E}{RT}\right] \exp\left[-\frac{\gamma(\omega_1 \hat{V}^* + \omega_2 \xi \hat{V}_2^*)}{\hat{V}_{FH}}\right] \quad (13)$$

Here D_0 is a constant preexponential factor, E is the energy per mole that a molecule needs to overcome attractive forces that hold it to its neighbor, T is temperature, γ is an overlap factor introduced to account for the fact that the same free volume is available to more than one molecule ($0.5 < \gamma < 1.0$), $\hat{V}_i^*$ is the specific critical hole volume of component i required for a jump, ξ is the ratio of the critical molar volume of the solvent jumping unit to the critical molar volume of the polymer jumping unit, and $\hat{V}_{FH}$ is the average hole free volume per gram of mixture, where the subscripts 1 and 2 designate the monomer and polymer, respectively. Finally, the term ξ can be calculated as

$$\xi = \hat{V}_1^* M_{j1} / \hat{V}_2^* M_{j2} \quad (14)$$

where M_{ji} is the molecular weight of a jumping unit of component i.

For cross-linked systems, Vrentas and Vrentas used the following equation for the calculation of $\hat{V}_{FH}$.

$$\hat{V}_{FH} = \omega_1 \hat{V}_{FH1} + \omega_2 \hat{V}_{FH2}(T,0)\, \delta \quad (15)$$

Here, $\hat{V}_{FHi}$ is the specific hole volume of pure component i at the temperature of interest, δ is the factor introduced to account for the presence of cross-links, and $\hat{V}_{FH2}(T,0)$ is the specific hole free volume for a corresponding uncross-linked polymer. The term δ is given by

$$\delta = \frac{\hat{V}_{FH2}(T,X)}{\hat{V}_{FH2}(T,0)} = \frac{\hat{V}_2^0(T,X)}{\hat{V}_2^0(T,0)} \quad (16)$$

where $\hat{V}_2^0(T,X)$ is the specific volume of the polymer at degree of cross-linking X.

As demonstrated by Kloosterboer,[1] during bulk cross-linking polymerization, the matrix volume shrinkage rate lags behind the reaction rate. This leads to the presence of a temporary excess free volume that is present during the reaction. As reaction rate is increased, the lag between the shrinkage and reaction rate increases, causing an increase in the temporary excess free volume and leading to a greater mobility of reacting species and a higher limiting conversion. This effect explains the higher final conversions obtained as the photoinitiation rate is increased as observed in our recent publication.[13]

This temporary excess free volume needs to be included in the calculation of the monomer diffusivity. This was done by adding an excess free volume term, $\hat{V}_{FHe}$, to the Vrentas–Vrentas calculation of $\hat{V}_{FH}$. Equation 15 was then rewritten as

$$\hat{V}_{FH} = \omega_1 \nu_m \upsilon_{fm} + \omega_2 \nu_p(T,0)\, \upsilon_{fp} \delta + \hat{V}_{FHe} \quad (17)$$

where $\hat{V}_{FHe}$ is the excess free volume per gram of the mixture and is calculated using the Bowman–Peppas treatment[10] as shown later, ν_m and ν_p are the specific volumes of the monomer and polymer, and υ_{fm} and υ_{fp} are the fractional free volumes of the monomer and polymer, respectively.

Equation 13 can now be used to estimate the diffusion coefficients of the monomer and the primary radicals in the polymerizing system. Predictive methods have been developed[41] to obtain all the parameters in the Vrentas–Vrentas theory.

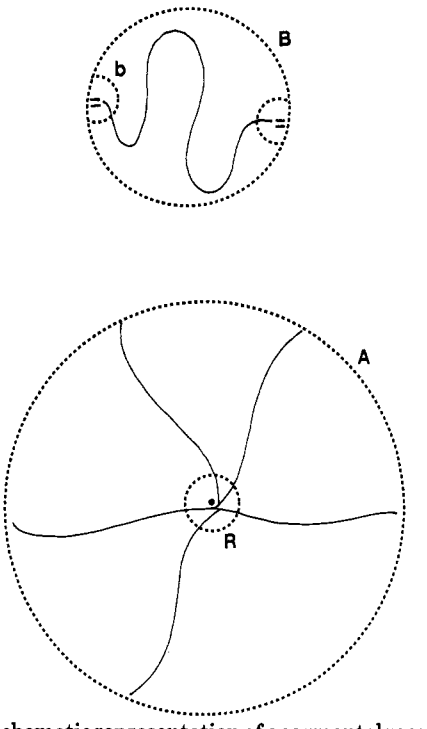

Figure 2. Schematic representation of a segmental reorientation process during propagation reactions. The radical is available for reaction in a volume R. However, not all of the surface area of sphere R is available for reaction because of spatial constraints induced by network chains. The monomer is represented as a sphere B of which the double bonds are effective over an area b. For reaction to occur, area b must overlap with the effective area of sphere R.

Thus, eq 11 can be used to calculate $k_{p,trans}$ throughout the polymerization reaction. As might be expected, as reaction proceeds and polymer is formed, the monomer diffusion coefficient decreases continuously, making further reactions proceed at a lower rate. On a molecular scale, the local diffusivity of the monomer near a radical site may be lower than the bulk monomer diffusivity as calculated by eq 13, but at present this effect is difficult to model and was not considered in the present analysis.

The segmental diffusion coefficient, D_{seg}, was estimated as

$$D_{seg} = pD_m \quad (18)$$

where p is the probability that one of the double bonds of the monomer is oriented toward the radical site. Such an approach allows for the estimation of D_{seg} especially at the onset of the reaction. The probability, p, was estimated using a technique of North.[42]

Figure 2 is a schematic representation of the segmental reorientation process. The monomer chain about to undergo a propagation reaction is encircled in a sphere B, with radius r_B. The double bonds of monomer are free to move on the surface of sphere B in an area of radius r_{db}. The polymer network containing the radical is contained in a sphere A, and the radical itself is allowed to have an effective reaction radius of r_R. Further, assume that sphere B undergoes rotational motion while sphere A is stationary.

If the double bonds on sphere B are moving with velocity υ_{db} and if sphere B flattens out as it approaches sphere R, then the area A_s projected by the double bonds in time τ_B is given by

$$A_s = 2(\pi r_{db}^2 + 2 r_{db} \upsilon_{db} \tau_B) \quad (19)$$

During time τ_B that sphere B is in contact with sphere R, the fraction of area B that is effective, p_b, is

$$p_b = \frac{2(\pi r_{db}^2 + 2r_{db}v_{db}\tau_B)}{4\pi r_B^2} \quad (20)$$

Since the radical is present at a cross-link point and surrounded by chains that are part of the network, only a fraction of the surface of sphere R will be actually accessible to the radical. In this analysis, the effective area of sphere R, p_r, was assumed to be 5%.

The term p was calculated as

$$p = p_r p_b = 0.05\left[\frac{1}{2}\left[\frac{r_{db}}{r_B}\right]^2 + \frac{1}{\pi}\frac{r_{db}}{r_B}\left[\frac{v_{db}\tau_B}{r_B}\right]\right] \quad (21)$$

The rotational diffusion coefficient is defined[43] as

$$D_{rot,B} = \theta_B^2/2\tau_B \quad (22)$$

where θ_B is the angular displacement given by

$$\theta_B = v_{db}\tau_B/r_B \quad (23)$$

If d_t is the length that sphere B flattens on collision with sphere R then,

$$\tau_B = d_t^2/6D_{trans,B} \quad (24)$$

where $D_{trans,B}$ is the translational diffusion coefficient of B.

The terms $D_{rot,B}$ and $D_{trans,B}$ can also be expressed as

$$D_{rot,B} = k_B T/8\pi\eta r_B^3 \quad (25)$$

and

$$D_{trans,B} = k_B T/6\pi\eta r_B \quad (26)$$

where k_B is the Boltzmann constant, T is temperature, and η is the solvent viscosity.

Using eqs 22–26, eq 21 was written as

$$p = \frac{0.05}{2}\left[\left[\frac{r_{db}}{r_B}\right]^2 + \frac{1}{\pi}\frac{r_{db}}{r_B}\frac{d_t}{r_B}\right] \quad (27)$$

Assuming $r_{db} = 0.1r_B$ and $d_t = 0.4r_B$, the probability p was estimated to be on the order of 10^{-4}. Then, eq 18 could be used in eq 12 to calculate the segmental diffusion contribution to k_p.

For linear polymerizations, previous studies[44] have shown that the segmental diffusion coefficient of active polymer chains does not change appreciably with conversion. The segmental diffusion coefficient of the monomer will exhibit this behavior even in a cross-linking polymerization. Hence, in this analysis, D_{seg} was maintained at a constant value calculated at the onset of the polymerization.

Termination. Termination occurs when two radicals are close enough that they will react and form a dead polymer chain. Since the radicals are present very near the cross-link points, it was assumed that after a few propagation steps, motion of the segment that contains the radical was severely limited. In this case, the only possible movement of the radical was due to propagation reactions; such diffusion is called "propagation diffusion" or "reaction diffusion".[45,46]

In each propagation step, the radical moves a distance of two bond lengths. When a sufficient number of propagation steps have taken place, the radical will have moved along a contour of a hypothetical polymer chain that has a constant bond length, and bond angle and rotation angle restrictions. The root mean square (rms) displacement, $\overline{r^2}$, can then be calculated as

$$\overline{r^2} = 2nl^2 \quad (28)$$

where n is the number of bonds and l is the bond distance.

The radical propagation diffusion coefficient, D_{rp}, was assumed to be Fickian and was calculated[47] as

$$D_{rp} = \overline{r^2}/6t_{\overline{r^2}} \quad (29)$$

where D_{rp} is the diffusivity of the radical due to propagation reactions and $t_{\overline{r^2}}$ is the time required for the radical to move a rms displacement of $\overline{r^2}$.

The time required for one propagation step, t_p, is given by

$$t_p = 1/k_p[M] \quad (30)$$

Therefore, the time required for the radical to undergo an rms displacement of $\overline{r^2}$ and travel over n bonds was given by

$$t_{\overline{r^2}} = \frac{n}{2}\frac{1}{k_p[M]} \quad (31)$$

From eq 29 and 31, we obtained

$$D_{rp} = \frac{2}{3}l^2 k_p[M] \quad (32)$$

Approaches similar to the one presented here have been used by other investigators.[48-50] Since the termination reaction was diffusion-limited, the Smoluchowski expression of eq 10 was again used to estimate the termination rate constant. Hence, k_t was expressed as

$$k_t = 4\pi(r_r + r_r)(D_{rp} + D_{rp}) \quad (33)$$

Using eqs 32 and 33, we obtained

$$k_t = \frac{32}{3}\pi r_r l^2 k_p[M] \quad (34)$$

Equation 34 was used to calculate the termination rate constant at all stages of conversion. This equation shows that when the propagation reaction stops due to diffusion limitations, no radical movement occurs, and the radicals are trapped.

Effect of Volume Relaxations. As shown by Bowman and Peppas,[10] the effect of volume relaxations on the reaction kinetics can be included in the model by expressing the rate of change of the specific volume of the system as proportional to its deviation from its equilibrium value. The proportionality constant is characteristic of the system and inversely proportional to the relaxation time so that

$$dv/dt = -(v - v_\infty)/\tau \quad (35)$$

Here, v is the specific volume, τ is the relaxation time, and v_∞ is the equilibrium specific volume calculated from the conversion as

$$v_\infty = v_m(1 - \epsilon_v x) \quad (36)$$

In the last equation, v_m is the specific volume of the monomer, x is conversion, and ϵ_v is the volume contraction factor calculated from the specific volumes of the monomer,

ν_m, and polymer, ν_p, as

$$\epsilon_v = (\nu_m - \nu_p)/\nu_m \quad (37)$$

The free-volume-dependent relaxation time was calculated as

$$\ln \tau = C_1 + C_2/v_f \quad (38)$$

where C_1 and C_2 are constants and v_f is the fractional free volume calculated as follows:

$$v_f = v_{fm}\phi_m + v_{fp}\phi_p + (\nu - \nu_\infty)/\nu_\infty \quad (39)$$

In the last expression, ϕ is the volume fraction, and the subscripts m and p stand for monomer and polymer, respectively. The last term in eq 39 accounts for the temporary excess volume due to the volume relaxation effects. It must be noted that v_{fp} is 0.025 since the polymer is in a glassy state, and v_{fm} was calculated at the reaction temperature using the relation given below.

$$v_{fm} = 0.025 + \alpha_m(T - T_{gm}) \quad (40)$$

Here, α_m is the difference in the thermal expansion coefficient when the polymer passes through the rubbery transition, T_{gm} is the glass transition temperature of the monomer, and T is the reaction temperature.

Finally, the excess free volume, $\hat{V}_{FHe}$, at any time was calculated as

$$\hat{V}_{FHe} = \nu - \nu_\infty \quad (41)$$

Equation 41 was used to calculate the excess hole free volume term, $\hat{V}_{FHe}$, in eq 17.

This completed the formal derivation of the model. Expressions were derived for the diffusion coefficient dependent initiator efficiency and propagation and termination rate constants. The translational diffusion coefficient of the monomer was calculated using the Vrentas–Vrentas theory modified to account for the presence of a temporary excess free volume. The derived expressions were incorporated into the rate equations (4) and (5) which were numerically integrated to obtain theoretical reaction rate profiles, conversion profiles, and other desired kinetic information.

Results and Discussion

Model simulations were performed to predict the behavior of bulk cross-linking photopolymerizations and to compare such results to the experimentally observed reaction characteristics. These simulations were carried out by numerically integrating the rate equations to obtain the polymerization rate profiles and other desired information. These predictions were compared with the kinetic behavior reported earlier[13] for the photopolymerizations of DEGDA monomer using 2,2-dimethoxy-2-phenylacetophenone as an initiator.

The parameters used in the simulations (see Table 1) were chosen so as to represent the characteristics of DEGDA bulk photopolymerization. The monomer and initiator concentrations were chosen to represent a reaction mixture containing DEGDA monomer and 1% photoinitiator. The monomer and polymer specific voluems were experimentally determined by us. Available literature values for the extinction coefficient,[10] the thermal expansion coefficient,[51] relaxation parameters,[10] and bond length[52] were used. The glass transition temperature of the monomer was set equal to that of tetraethylene glycol diacrylate.[53] Monomer and radical reaction radii were estimated from their Lennard-Jones diameters.[54] The

Table 1. Values of the Parameters Used in the Numerical Integrations of the Rate Equations (4) and (5)

ϵ (L/mol·cm)	100	$[A]_0$ (M)	0.047
$[M]_0$ (M)	10.48	T (°C)	30
α_m (K^{-1})	0.001	T_{gm} (°C)	−60
v_{fp}	0.025	ν_p (cm^3/g)	0.8
ν_m (cm^3/g)	0.9		
C_1	0.5	C_2	0.165
r_m (Å)	3	r_r (Å)	1.5
l (Å)	1.54		
D_0 (monomer) (cm^2/s)	44	E (cal/mol)	9253
R (cal/mol·K)	1.987	D_0 (radical) (cm^2/s)	440
$\hat{V}_1^*$ (cm^3/g)	0.5	$\hat{V}_2^*$ (cm^3/g)	0.9
ξ	0.9	δ	0.94
γ	0.9		
ϕ'	1	$k_{i,1}$ (cm/s)	1.32×10^3
$k_{d,r,1}$ (s^{-1})	10^{11}	a (Å)	10
$k_{p,1}$ (L/mol·s)	10^8		

Vrentas–Vrentas diffusion theory[39,40] parameters were evaluated from the predictive methods presented by Zielinski and Duda.[41] The initiator decomposition reaction parameters have been previously determined by us.[33] Since ϕ is typically between 0.3 and 0.8, ϕ' was determined to be unity. None of the parameters were used for fitting the experimental data.

Figure 3 shows the reaction rate as a function of time obtained by performing the numerical integration of the rate expressions using a light intensity of 0.02 mW/cm². The reaction rate was plotted as a percent of the initial number of double bonds reacted per second. This profile indicates all the experimentally observed reaction trends recorded during the photopolymerization of DEGDA when a light intensity of 0.02 mW/cm² was used.[13] The polymerization was initially rapid, and the reaction rate fell to one-hundredth of its maximum value in about 135 s. Such a sharp increase followed by a decrease in the reaction rate indicated the presence of autoacceleration and autodeceleration caused by a decrease in the propagation and termination rate constants during the course of the polymerization.

Such changes in the rate constants were observed in the calculated values of k_p and k_t. Figure 4 shows the theoretical values of k_p and k_t as a function of reaction time when a light intensity of 0.02 mW/cm² was used for initiation. The value of k_t at the onset of the reaction seems low when compared to that typical of linear and some cross-linking polymerizations. This is partly because the chemical step often controls the termination reaction mechanism at the onset of these polymerizations. However, in the case of multifunctional homopolymerizations such as those considered in this paper, propagation diffusion becomes and remains the dominant mode of termination usually before 5% conversion is attained.[55] Some experimental evidence indicates that values as low as 10^3 L/mol·s are possible when propagation diffusion is the controlling mechanism for termination reactions.[55]

This figure shows that k_t decreased from the onset of the reaction while k_p remained constant; such behavior causes autoacceleration. The rate constant k_p remained constant when segmental diffusion controlled the polymerization but began to decrease as translational diffusion became the controlling step. In the late stages of the polymerization reaction, the calculated values of the termination and the propagation rate constants were similar because propagation diffusion was the only mode available for radical movement.

An increase in the theoretical value of the radical concentration was observed immediately after photoinitiation as can be seen in Figure 5 for photopolymerizations with UV light of intensity 0.02 mW/cm². The fast increase implied that the rate of initiation, R_i, was greater than the

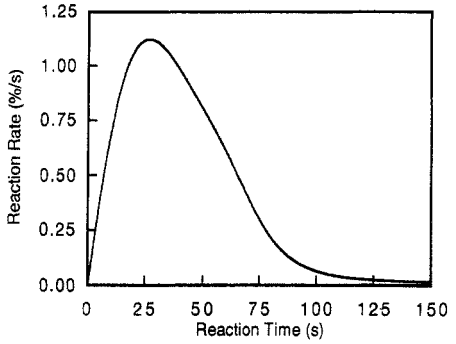

Figure 3. Theoretical values of the DEGDA photopolymerization rate as a function of time when UV light of intensity 0.02 mW/cm² was used to initiate the photopolymerization. The reaction rate is plotted as the percent of the initial number of acrylic double bonds reacted per second.

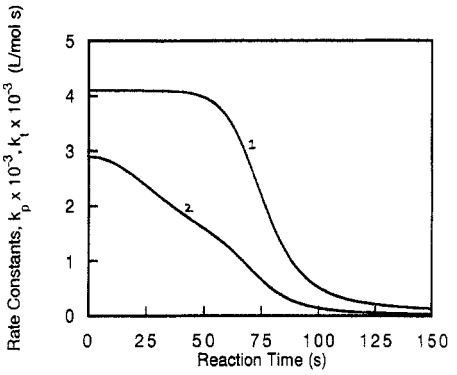

Figure 4. Theoretical values of the propagation and termination rate constants, k_p (curve 1) and k_t (curve 2), as a function of time when a light intensity of 0.02 mW/cm² was used for photoinitiation.

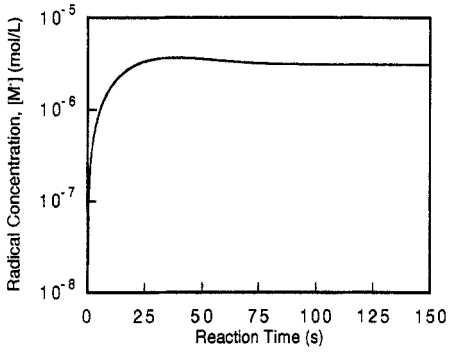

Figure 5. Theoretical values of the radical concentration as a function of polymerization time at an incident UV light intensity of 0.02 mW/cm². The steady-state level during the latter stages of the reaction indicated the presence of trapped radicals.

rate of termination, R_t (see eq 4). This was because initially the quantum yield for initiation was at a high value, thus contributing to a high R_i, and, although k_t too had a significant value, the radical concentration was low, leading to a low termination rate. Therefore, this rapid increase in the radical concentration at the onset was mainly due to the formation of radicals that initiate propagating chains. Some contribution to this increase may have been the result of a slight decrease in k_t.

After the sharp increase, between 35 and 40 s, the radical concentration profile levels off, indicating that R_i was comparable to R_t. This was confirmed by verifying that the ratio of the rate of change of radical concentration to the initiation rate, $(d[M^\cdot]/dt)/R_i$, approached zero during this period.

Between 40 and 70 s, the radical concentration decreased slightly because the rate of termination was greater than the initiation rate. At the end of this period, k_t still had

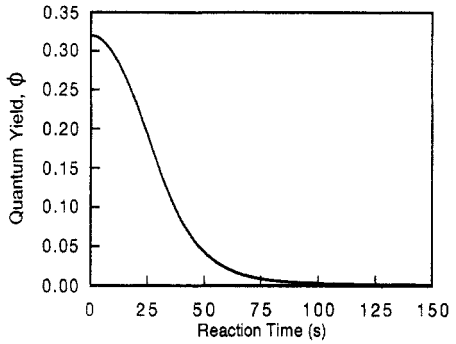

Figure 6. Theoretical values of the quantum yield of initiation, ϕ, as a function of reaction time during a reaction initiated with UV light of intensity 0.02 mW/cm². Since $\phi = f\phi'$, where ϕ' is a constant, the plot also demonstrates the decrease in the initiator efficiency, f.

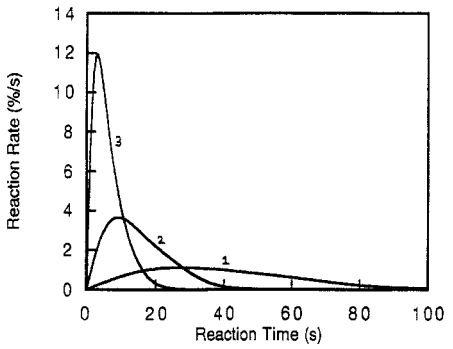

Figure 7. Theoretical values of the polymerization rate of DEGDA as a function of reaction time at three UV light intensities: 0.02 (curve 1), 0.2 (curve 2), and 2 mW/cm² (curve 3). The polymerization rate is shown as a percent of the initial number of acrylic double bonds consumed per second. An increase in the light intensity increased the initial and peak reaction rate.

a significant value as compared with its value at the onset of the reaction, while ϕ had dropped to one-tenth of its initial value as is shown later in Figure 6. This meant that while bimolecular termination reactions were still occurring (since the radical concentration was high), the rate of initiation had decreased during this period.

After approximately 90 s, the radical concentration began to level off and approach a steady-state value and remained there throughout the polymerization process. This occurred because in the late stages of the polymerization process, diffusion limitations caused the initiator efficiency to approach a limiting value of zero, thus causing the rate of initiation to be zero, and k_t decreased to a low value so that the rate of radical destruction was negligible. The constant value of the radical concentration indicated the presence of a trapped radical population. Such trapped radicals have long lifetimes[1,56] and lead to structural heterogeneities in the cross-linked networks.[9]

The new model incorporates a diffusion-dependent initiator efficiency, f. Indeed a plot of the quantum yield of initiation, ϕ, as a function of polymerization time (Figure 6) shows the decrease in f with time and, therefore, with conversion. The initiator efficiency decreased during the course of polymerization and attained a value about one-tenth of its initial value in 70 s. Such a sharp decrease in f has been reported[9] for azobis(isobutyronitrile)-initiated methyl methacrylate polymerizations. During the late stages of the reaction, the rate of chain initiation was negligible since most of the radicals formed on initiator decomposition recombined to form inactive initiator molecules.

Figure 7 shows the predicted reaction rates as a function of time using three light intensities: 0.02, 0.2, and 2 mW/

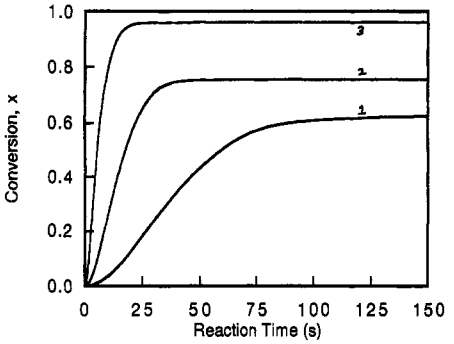

Figure 8. Theoretical conversion of acrylic double bonds as a function of time during the polymerization of DEGDA at UV light intensities of 0.02 (curve 1), 0.2 (curve 2), and 2 mW/cm^2 (curve 3). A slight S-shaped profile was observed at low light intensities demonstrating autoacceleration. As light intensity was increased, the limiting conversion increased because of the effect of volume relaxations. However, in each case, the limiting conversion was below 100% because of diffusional limitations on the reacting species.

cm^2. The model solutions showed an increase in reaction rate with an increase in light intensity. The rapidity of diacrylate photopolymerizations was indicated by the model, as was the strong autoacceleration phenomenon observed at each of the light intensities used to initiate the reaction. Both the initial and peak reaction rates increased with an increase in light intensity as a result of an increase in the rate of radical formation. Such trends have been experimentally observed.[13]

Conversion profiles for photoinitiation with UV light of intensities 0.02, 0.2, and 2 mW/cm^2 are shown in Figure 8. At low light intensities, an S-shaped curve was obtained indicative of a gel effect. As light intensity was increased, the final conversion increased and the time required for the limiting conversion to be reached decreased. However, in each case, the final conversion was less than 100%. This is because, as the polymer network is formed, the diffusivity of the reacting species falls to a point where no further reaction can occur within the time scale of the experiment. The final conversion increased with an increase in light intensity as a result of volume relaxations.

A comparison of theoretical values with experimental results previously reported by us[13] is shown in Table 2. These comparisons are presented for photopolymerizations at the three light intensities used in the experimental study. As the light intensity was increased from 0.02 to 2 mW/cm^2, the time at which the peak reaction rate was observed decreased from 24.3 to 4.1 s, and the induction time decreased from 5.8 to 1.5 s. The induction time was defined as the time required for 1% conversion so as to obtain an indication of the initial reaction rates. Theoretical predictions of these times were in agreement with the experimentally observed values.

The conversion at the reaction rate peak was predicted rather well by the theoretical model. The simulations showed a slight increase in these values as light intensity was increased, while the experimental results did not show this trend clearly. The peak heat flow rate increased as light intensity was increased. This occurred because of the increase in the number of radicals in the reacting system caused by an increase in the photoinitiation rate. The theoretical values of the peak heat flow rates were calculated by using a theoretical exothermic reaction enthalpy of 86.1 kJ per acrylic double bond.[57] The model was successful in predicting the increase in peak heat flow rate though underpredictions were observed at light intensities of 0.02 and 0.2 mW/cm^2.

Volume relaxation effects lead to a greater mobility of the reacting species at higher light intensities which lead to higher final conversions. Such an effect was observed in the experimental results shown in Table 2 where the final conversion increased from 53.7% at 0.02 mW/cm^2 to 94.0% at 2 mW/cm^2. The model predicted an increase in the limiting conversion value from 62.4% at 0.02 mW/cm^2 to 96.1% at 2 mW/cm^2, thus demonstrating that the effect of volume relaxations was satisfactorily accounted for in the model.

In general, the theoretical model tends to overpredict the limiting conversions. One of the reasons for this overprediction may be the calculation of the monomer diffusion coefficient using a theory applied only to lightly cross-linked systems.[34] Yet, the network formed toward the end of the reaction is a highly cross-linked one with an associated drastic reduction in monomer mobility. Model predictions for limiting conversions can be improved by employing a parameter in the Vrentas–Vrentas model that would cause a steeper decrease in the diffusion coefficient as the polymer weight fraction increases. Another reason for the overprediction may be that the model describes a reaction scheme where chain-transfer reactions are absent or suppressed. However, these reactions are present in acrylate polymerizations, thus imparting additional mobility to the radicals and decreasing the polymerization rate.[1]

The presence of unreacted monomer in the polymerized material is usually undesirable because the unreacted monomer serves as a plasticizer and decreases the mechanical strength, thermal stability, and structural integrity of the material. This is usually avoided by using high photoinitiation rates and increasing the final conversions. However, the simulation results showed that higher light intensities could lead to greater structural heterogeneities. These predictions are shown in Figure 9 in which the radical concentration was plotted as a function of time for the three light intensities used. As light intensity was increased, the steady-state level of radical concentration increased pointing to the existence of a larger number of trapped radicals at higher light intensities. This implies the presence of greater structural heterogeneities in materials prepared at high light intensities.

Conclusions

A kinetic model has been developed that reflects the transport processes occurring during a diffusion-limited bulk cross-linking photopolymerization. This model accounted for the change in the initiator efficiency with conversion as well as the lag of the volume shrinkage rate with respect to the reaction rate. These phenomena have

Table 2. Comparison of Model Predictions with Experimental Results[13] from Photopolymerizations at Three Light Intensities

	I_0 = 0.02 mW/cm^2		I_0 = 0.2 mW/cm^2		I_0 = 2 mW/cm^2	
param	expt	model	expt	model	expt	model
time for peak reaction rate (s)	24.3	27.0	9.3	9.0	4.1	3.0
induction time (s)	5.8	5.0	2.8	2.0	1.5	0.5
reacted at peak (%)	21.2	20.4	23.4	22.5	22.6	25.2
peak reaction rate (W/g)	13	9	42	30	98	96
final conversion (%)	53.7	62.4	67.6	75.6	94.0	96.1

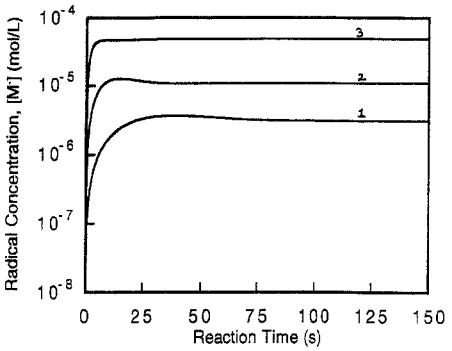

Figure 9. Theoretical values of the radical concentration as a function of time for DEGDA photopolymerizations at three UV light intensities: 0.02 (curve 1), 0.2 (curve 2), and 2 mW/cm^2 (curve 3). An increase in the steady-state value with an increase in light intensity indicated an increase in the number of trapped radicals and structural heterogeneities.

usually been ignored in previous modeling efforts. All the parameters in the model were fundamental quantities with physical significance, and hence this model has the capability of being used as a predictive tool.

The simulations carried out using the developed model demonstrated that this model could predict the experimentally observed reaction trends at varying light intensities. An increase in the light intensity caused an increase in the initial reaction rates and peak reaction rates. The effect of volume relaxations was satisfactorily incorporated into the model as was demonstrated by the fact that the simulated limiting conversions increased with an increase in light intensity.

The termination rate constant decreased from the onset of the reaction, contributing to autoacceleration. The radical concentration initially increased sharply and at long times maintained a steady-state level as a result of the fact that diffusional limitations caused the initiator efficiency and the termination rate constant to attain a very low value. The steady-state radical concentration indicated a trapped radical concentration which was greater when higher light intensities were used for the photopolymerizations.

Acknowledgment. We thank Dr. J. G. Kloosterboer of the Philips Research Laboratories in Eindhoven, The Netherlands, for helpful comments. This work was presented in part at the American Chemical Society Meeting, Chicago, IL, Aug 1993, and at the Annual American Institute of Chemical Engineers Meeting, St. Louis, MO, Nov 1993. This work was supported by a grant from the National Science Foundation (Grant No. CTS-93-11563) and a Global Initiative Faculty Grant from Purdue University.

References and Notes

(1) Kloosterboer, J. G. *Adv. Polym. Sci.* **1988**, *84*, 1.
(2) Kloosterboer, J. G.; Lippits, G. J. M.; Meinders, H. C. *Philips Tech. Rev.* **1982**, *40*, 298.
(3) Kloosterboer, J. G.; Lippits, G. J. M. *J. Radiat. Curing* **1984**, *11* (1), 10.
(4) Bowen, R. L. *J. Dent. Res.* **1970**, *49*, 810.
(5) Turner, D. T.; Haque, Z. U.; Kalachandra, S.; Wilson, T. W. *Polym. Mater. Sci. Eng. Proc.* **1987**, *56*, 769.
(6) Ruyter, I. E.; Oysaed, H. *Crit. Rev. Biocompat.* **1988**, *40*, 247.
(7) Odian, G. *Principles of Polymerization*, 3rd ed.; John Wiley & Sons: New York, 1992.
(8) Russell, G. T.; Napper, G. H.; Gilbert, R. G. *Macromolecules* **1988**, *21*, 2141.
(9) Shen, J. C.; Tian, Y.; Wang, G. B.; Yang, M. L. *Sci. China, Ser. B* **1990**, *33*, 1046.
(10) Bowman, C. N.; Peppas, N. A. *Macromolecules* **1991**, *24*, 1914.
(11) Zhu, S.; Tian, Y.; Hamielec, A. E.; Eaton, D. R. *Polym.* **1990**, *31*, 154.
(12) Decker, C.; Moussa, K. *J. Polym. Sci., Polym. Chem. Ed.* **1987**, *25*, 739.
(13) Kurdikar, D. L.; Peppas, N. A. *Polymer* **1994**, *35*, 1004.
(14) Bowman, C. N.; Peppas, N. A. *J. Appl. Polym. Sci.* **1991**, *42*, 2013.
(15) Marten, F. L.; Hamielec, A. E. In *Polymerization Reactors and Processes*; Henderson, J. N., Bouton, T. C., Eds.; ACS Symposium Series 104; American Chemical Society: Washington, DC, 1979; p 43.
(16) Chern, C. S.; Poehlein, G. W. *Polym. Plast. Technol. Eng.* **1990**, *29*, 577.
(17) Soh, S. K.; Sundberg, D. C. *J. Polym. Sci., Polym. Chem. Ed.* **1982**, *20*, 1299.
(18) Soh, S. K.; Sundberg, D. C. *J. Polym. Sci., Polym. Chem. Ed.* **1982**, *20*, 1315.
(19) Soh, S. K.; Sundberg, D. C. *J. Polym. Sci., Polym. Chem. Ed.* **1982**, *20*, 1331.
(20) Soh, S. K.; Sundberg, D. C. *J. Polym. Sci., Polym. Chem. Ed.* **1982**, *20*, 1345.
(21) Batch, G.; Macosko, C. *J. Appl. Polym. Sci.* **1992**, *44*, 1711.
(22) Manneville, P.; de Seze, L. In *Numerical Methods in the Study of Critical Phenomena*; Dora, J. D., Demongeot, J., Lacolle, B., Eds.; Springer: Berlin, 1981; p 116.
(23) Romiszowski, R.; Kolinsky, A. *Polymer* **1982**, *23*, 1226.
(24) Boots, H. M. J.; Pandey, R. B. *Polym. Bull.* **1984**, *11*, 415.
(25) Boots, H. M. J.; Kloosterboer, J. G.; Van de Hei, G. M. M.; Pandey, R. B. *Br. Polym. J.* **1985**, *17*, 219.
(26) Boots, H. M. J. In *Biological and Synthetic Polymer Networks*; Kramer, O., Ed.; Elsevier: Amsterdam, The Netherlands, 1988; p 267.
(27) Simon, G. P.; Allen, P. E. M.; Bennett, D. J.; Williams, D. R. G.; Zheng, Y. G. *Macromolecules* **1989**, *22*, 3555.
(28) Bansil, R.; Herrmann, H. J.; Stauffer, D. *Macromolecules* **1984**, *17*, 998.
(29) Bowman, C. N.; Peppas, N. A. *Chem. Eng. Sci.* **1992**, *46*, 1411.
(30) Sandner, M. R.; Osborn, C. L. *Tetrahedron Lett.* **1974**, *5*, 415.
(31) Borer, A.; Kirchmayer, R.; Rist, G. *Helv. Chim. Acta* **1978**, *61*, 305.
(32) Groenenboom, C. J.; Hageman, H. J.; Overeem, T.; Weber, A. J. M. *Makromol. Chem.* **1982**, *183*, 281.
(33) Kurdikar, D. L.; Peppas, N. A. *Macromolecules* **1994**, *27*, 733.
(34) Vrentas, J. S.; Vrentas, C. M. *J. Appl. Polym. Sci.* **1991**, *42*, 1931.
(35) Rice, S. In *Diffusion-Limited Reactions*; Bamford, C. H., Tipper, C. F. H., Compton, R. G., Eds.; Elsevier: New York, 1985; p 3.
(36) Tulig, T. J.; Tirrell, M. *Macromolecules* **1981**, *14*, 1501.
(37) Ito, K. *Polym. J.* **1980**, *12*, 499.
(38) Ito, K. *Polym. J.* **1984**, *16*, 761.
(39) Vrentas, J. S.; Duda, J. L. *J. Polym. Sci., Polym. Phys. Ed.* **1977**, *15*, 403.
(40) Vrentas, J. S.; Duda, J. L. *J. Polym. Sci., Polym. Phys. Ed.* **1977**, *15*, 417.
(41) Zielinski, J. M.; Duda, J. L. *AIChE J.* **1992**, *38*, 405.
(42) North, A. M. *Makromol. Chem.* **1965**, *83*, 15.
(43) Einstein, A. In *Investigations on the Theory of Brownian Movement*; Furth, R., Ed.; Metheun: London, 1926; p 32.
(44) Mahabadi, H. K.; O'Driscoll, K. F. *Macromolecules* **1977**, *10*, 55.
(45) Stickler, M. *Makromol. Chem.* **1983**, *184*, 2563.
(46) Stickler, M.; Panke, D.; Hamielec, A. E. *J. Polym. Sci., Polym. Phys. Ed.* **1984**, *22*, 2243.
(47) Chandrasekhar, S. *Rev. Mod. Phys.* **1943**, *15*, 1.
(48) Russell, G. T.; Napper, G. H.; Gilbert, R. G. *Macromolecules* **1988**, *21*, 2133.
(49) Mills, M. F.; Gilbert, R. G.; Napper, D. H. *Macromolecules* **1990**, *23*, 4247.
(50) Dube, M. A.; Rilling, K.; Pendilis, A. *J. Appl. Polym. Sci.* **1991**, *43*, 2137.
(51) Ferry, J. D. *Viscoelastic Properties of Polymers*; John Wiley and Sons: New York, 1980.
(52) Flory, P. J. *Principles of Polymer Chemistry*; Cornell University Press: Ithaca, NY, 1953.
(53) Kloosterboer, J. G.; Lijten, G. F. C. M. *Polym. Mater. Sci. Eng. Proc.* **1988**, *56*, 759.
(54) Bird, R. B.; Stewart, W. E.; Lightfoot, E. N. *Transport Phenomena*; John Wiley and Sons: New York, 1960.
(55) Anseth, K. S.; Bowman, C. N.; Peppas, N. A. *J. Polym. Sci., Polym. Chem. Ed.* **1994**, *32*, 139.
(56) Scranton, A. B.; Bowman, C. N.; Klier, J.; Peppas, N. A. *Polymer* **1992**, *33*, 1683.
(57) Moore, J. E. In *Chemistry and Properties of Crosslinked Polymers*; Labana, S. S., Ed.; Academic Press: New York, 1977; p 535.